

# VLQBounds: Confronting Vector-Like Quark Models with LHC Searches

A. Arhrib<sup>a,b</sup>, R. Benbrik<sup>c</sup>, M. Boukidi<sup>d</sup>, M. Ech-chaouy<sup>c</sup>, S. Moretti<sup>e,f</sup>, K.  
Kahime<sup>g</sup>, K. Salime<sup>c</sup>, Q.S. Yan<sup>h,i</sup>

<sup>a</sup>*Abdelmalek Essaadi University, FST Tanger B.P. 416, Morocco*

<sup>b</sup>*LAPTh, CNRS, Université Savoie Mont-Blanc, 9 Chemin de Bellevue, 74940, Annecy,  
France*

<sup>c</sup>*Polydisciplinary Faculty, Laboratory of Physics, Energy, Environment, and  
Applications, Cadi Ayyad University, Safi, Morocco*

<sup>d</sup>*Institute of Nuclear Physics, Polish Academy of Sciences, ul. Radzikowskiego 152,  
Cracow 31-342, Poland*

<sup>e</sup>*Department of Physics & Astronomy, Uppsala University, SE-751 20 Uppsala, Sweden*

<sup>f</sup>*School of Physics & Astronomy, University of Southampton, Southampton SO17 1BJ,  
United Kingdom*

<sup>g</sup>*Laboratoire Interdisciplinaire de Recherche en Environnement, Management, Energie et  
Tourisme (LIREMET), ESTE, Cadi Ayyad University, B.P. 383, Essaouira, Morocco*

<sup>h</sup>*Center for Future High Energy Physics, Chinese Academy of Sciences, Beijing 100049,  
China*

<sup>i</sup>*School of Physics Sciences, University of Chinese Academy of Sciences, Beijing 100039,  
China*

---

## Abstract

We present VLQBounds, a public, data-driven Python framework for testing Vector-Like Quark (VLQ) scenarios against Large Hadron Collider (LHC) exclusion limits from ATLAS and CMS. The framework incorporates public results on both pair and single VLQ production and supports the main parameterisations used in experimental interpretations, including mass-mixing, mass-coupling, and mass-width representations. For each parameter point, the predicted cross-section or effective coupling is compared channel by chan-

---

*Email addresses:* aarhrib@gmail.com (A. Arhrib), r.benbrik@uca.ac.ma (R. Benbrik), mohammed.boukidi@ifj.edu.pl (M. Boukidi), m.echchaouy.ced@uca.ac.ma (M. Ech-chaouy), stefano.moretti@physics.uu.se (S. Moretti), s.moretti@oton.ac.uk (S. Moretti), Kahimek@gmail.com (K. Kahime), k.salime.ced@uca.ac.ma (K. Salime), yanqishu@ucas.ac.cn (Q.S. Yan)

nel to the corresponding observed and expected experimental limits through interpolation over machine-readable grids. The most sensitive analysis is automatically identified and a 95% Confidence-Level exclusion verdict is returned, together with the observed and expected sensitivity ratios and the metadata needed for reproducible reinterpretation. The modular structure of VLQBounds makes it suitable for fast phenomenological scans, validation of public limits, and future extensions to new collider searches and non-minimal VLQ decay patterns.

*Keywords:* Vector-Like Quarks, LHC, reinterpretation, exclusion limits, recasting, reproducible workflows

---

## 1. Introduction

The exploration of physics Beyond the Standard Model (BSM) remains a central focus of the high-energy physics programme at the LHC. Despite its remarkable successes, the SM does not address several open questions, including the origin of the fermion mass hierarchy, the detailed structure of Electro-Weak Symmetry Breaking (EWSB), the presence of Dark Matter (DM), and the mechanism behind the observed matter-antimatter asymmetry in the Universe. Among the most actively studied classes of extensions are models that introduce VLQs, hypothetical spin-1/2 fermions whose left- and right-handed components transform identically under the SM gauge group [1–4].

Such VLQs arise naturally in a variety of ultraviolet completions, including Composite Higgs Models (CHMs) [5, 6], Little Higgs constructions [7, 8], extra-dimensional scenarios [9, 10], and Grand Unified Theories (GUTs) with extended gauge symmetries [11]. Beyond these frameworks, the phenomenology of VLQs has also been extensively investigated in the context of the Two-Higgs-Doublet Model (2HDM) [12–22]. Their vector-like character of these new fermions permits gauge-invariant mass terms independently of EWSB and without necessarily destabilising precision EW constraints. Depending on their mixing with SM quarks, VLQs can modify Higgs and EW couplings, induce flavour-non-universal signatures, and motivate a broad experimental search programme.

At the LHC, VLQs are produced mainly through two complementary mechanisms. Pair production proceeds through QCD interactions and is largely model-independent, depending primarily on the VLQ mass. Single production proceeds through EW interactions and is directly sensitive to the mixing or effective coupling between the heavy fermion and SM quarks. ATLAS and CMS have searched for the four canonical VLQ states, namely the up-type partner  $T$ , the down-type partner  $B$ , and the exotic partners  $X$  and  $Y$ , across a wide range of final states. The resulting constraints now reach the TeV scale in several channels [23, 24].

The reinterpretation of these results is not straightforward. Experimental limits are published in several native forms: upper bounds on cross-sections, exclusion contours in the  $(m_Q, \sin \theta_{L/R})$  plane, limits in the  $(m_Q, \kappa)$  one, and bounds in the  $(m_Q, \Gamma_Q/m_Q)$  one under fixed Branching Ratio (BR) assumptions. The diversity of representations, topologies, and assumptions makes it difficult to test arbitrary VLQ scenarios in a coherent and automated way, especially when scanning large parameter spaces or studying non-minimal representations.

Public tools directly tailored to VLQ interpretations are still relatively scarce. The closest dedicated public code is XQCAT, which determines exclusion confidence levels for scenarios with one or several extra quarks by relying on precomputed efficiencies for QCD pair production and on-shell decays [25]. More general public reinterpretation frameworks, such as MadAnalysis 5, CheckMATE, SModelS, Fastlim, and Contur, can also be used to confront BSM scenarios with collider data [26–30]. However, these tools are not organised around the native  $(m_Q, s_{L/R})$ ,  $(m_Q, \kappa)$ , and  $(m_Q, \Gamma_Q/m_Q)$  representations in which VLQ limits are often presented. In this sense, VLQBounds is designed as a dedicated and lightweight layer for the direct use of public VLQ searches, while remaining complementary to broader recasting infrastructures.

To address this issue, we introduce VLQBounds, a Python framework that compares theoretical predictions for VLQ models with public ATLAS and CMS exclusion limits. The framework handles the standard VLQ species  $T$ ,  $B$ ,  $X$ , and  $Y$ , including singlet, doublet, triplet, and fixed BR configurations. It accepts input in terms of masses, mixing angles, effective couplings, and/or relative widths and performs the required translations internally. For

each model point, VLQBounds evaluates the relevant observables, interpolates the experimental limits in their native variables, identifies the most sensitive analysis, and returns a 95% CL exclusion decision together with the corresponding diagnostic information.

The code is intended for parameter scans and validation studies. It includes an interface for reproducing published mass-width and mass-coupling exclusion plots directly from the internal VLQBounds data files, without hard-coding numerical inputs in external scripts. The same internal workflow is used for validation plots and scan outputs.

The paper is organised as follows. Section 2 summarises the theoretical setup and conventions. Section 3 describes the exclusion methodology. Section 4 summarises the experimental inputs. Section 5 details the software architecture, public API, scan interface, and validation plotting tools. Section 6 presents validation examples while Sec. 7 gives representative applications. Conclusions are presented in Sec. 8.

## 2. Model Framework and Notation

Here, we summarise only the conventions required by VLQBounds (a complete derivation of the mass matrices, mixing structure, and gauge/Higgs interactions can be found in Ref. [23]. With an  $SU(2)_L$  doublet scalar sector and renormalisable quark-VLQ mixings, the admissible gauge-covariant multiplets are [31]

$$\begin{aligned}
T_{L,R}^0, \quad B_{L,R}^0 & && \text{(singlets),} \\
(X T^0)_{L,R}, \quad (T^0 B^0)_{L,R}, \quad (B^0 Y)_{L,R} & && \text{(doublets),} \\
(X T^0 B^0)_{L,R}, \quad (T^0 B^0 Y)_{L,R} & && \text{(triplets).} \quad (1)
\end{aligned}$$

The states  $Q = \{T, B\}$  carry electric charges  $\{+2/3, -1/3\}$ , while the exotic partners  $X$  and  $Y$  carry  $+5/3$  and  $-4/3$ , respectively. We restrict the treatment to one additional VLQ multiplet mixing dominantly with the third SM generation.

*Mixing Conventions.* In the up- and down-type sectors, weak and mass eigenstates are related by  $2 \times 2$  unitary rotations  $U_{L,R}^q$  with angles  $\theta_{L,R}^q$ .

We use  $s_{L,R}^q \equiv \sin \theta_{L,R}^q$  and  $c_{L,R}^q \equiv \cos \theta_{L,R}^q$ . For singlets and triplets the dominant mixing is left-handed, while for doublets it is right-handed. The subdominant angle is fixed by [1]

$$\tan \theta_R^q = \frac{m_q}{m_Q} \tan \theta_L^q \quad (\text{singlets, triplets}), \quad \tan \theta_L^q = \frac{m_q}{m_Q} \tan \theta_R^q \quad (\text{doublets}), \quad (2)$$

with  $(q, m_q, m_Q) = (u, m_t, m_T)$  or  $(d, m_b, m_B)$ . Complex phases are neglected, since they are not relevant for the exclusion logic implemented here.

*Decays and Working Assumptions.* In the minimal SM+VLQ limit, where no additional light BSM states enter the decay chain, the partial widths are determined by the gauge and Higgs interactions fixed by the mixing angles. The standard decay patterns are

$$T \rightarrow W^\pm b, Zt, ht, \quad B \rightarrow W^\pm t, Zb, hb, \quad X \rightarrow W^\pm t, \quad Y \rightarrow W^\pm b.$$

When an experimental analysis is published under fixed BR assumptions, VLQBounds uses those assumptions only for the corresponding comparison.

*Input Parameterisations.* For each VLQ species, the framework accepts one of the following inputs:

$$(m_Q, s_{L/R}), \quad (m_Q, \kappa), \quad (m_Q, \Gamma_Q/m_Q).$$

Theory predictions for production and decays are evaluated accordingly. When necessary, the code translates between these representations using the relations in Table 1.

*Masses and Multiplet Consistency.* By default, VLQBounds treats the masses of the different VLQ species as independent user-specified inputs. The conventions above are sufficient to map arbitrary points in VLQ parameter space onto ATLAS and CMS limit grids in their native variables, whether cross-section,  $(m_Q, s_{L/R})$ ,  $(m_Q, \kappa)$ , or  $(m_Q, \Gamma_Q/m_Q)$ . Full details of the interaction Lagrangian, mixing structure, and diagonalisation conventions are given in Ref. [23].

VLQ representation	Model	Translation: $\kappa$ in terms of mixing
$T$	Singlet	$\sqrt{2} s_L$
	Doublet $(X, T)$	$s_R c_R$
	Doublet $(T, B)$	$s_R^u c_R^u$
$B$	Singlet	$\sqrt{2} s_L$
	Doublet $(B, Y)$	$s_R c_R$
	Doublet $(T, B)$	$s_R^d c_R^d$
$X$	Doublet $(X, T)$	$s_R$
$Y$	Doublet $(B, Y)$	$s_R$
$Y$	Triplet $(T, B, Y)$	$\sqrt{2} s_L^d$

Table 1: Map between the experimental coupling parameter  $\kappa$  and the dominant quark-VLQ mixing angles used in this work.

### 3. VLQBounds Approach

The absence of experimental evidence for VLQs at the LHC is translated into constraints on their production and decay rates. These constraints are usually expressed as upper limits on cross-sections for processes in which VLQs are produced and subsequently decay into experimentally accessible final states. Two production mechanisms are central: pair production and single production.

Pair production,  $pp \rightarrow Q\bar{Q}$ , is driven by QCD interactions and is therefore largely independent of the detailed VLQ mixing pattern. The theoretical prediction depends predominantly on the VLQ mass, making pair production the natural baseline for model-independent exclusions. Experimental upper bounds on  $\sigma(pp \rightarrow Q\bar{Q})$  can therefore be recast into lower limits on  $m_Q$  under specified BR hypotheses.

Single production, by contrast, is mediated by EW interactions and depends on both the VLQ mass and effective couplings to SM quarks. The corresponding limits are therefore interpreted in a two-dimensional space, typically  $(m_Q, \kappa)$  or  $(m_Q, \Gamma_Q/m_Q)$ . Representative single- and pair-production topologies are shown in Fig. 1.

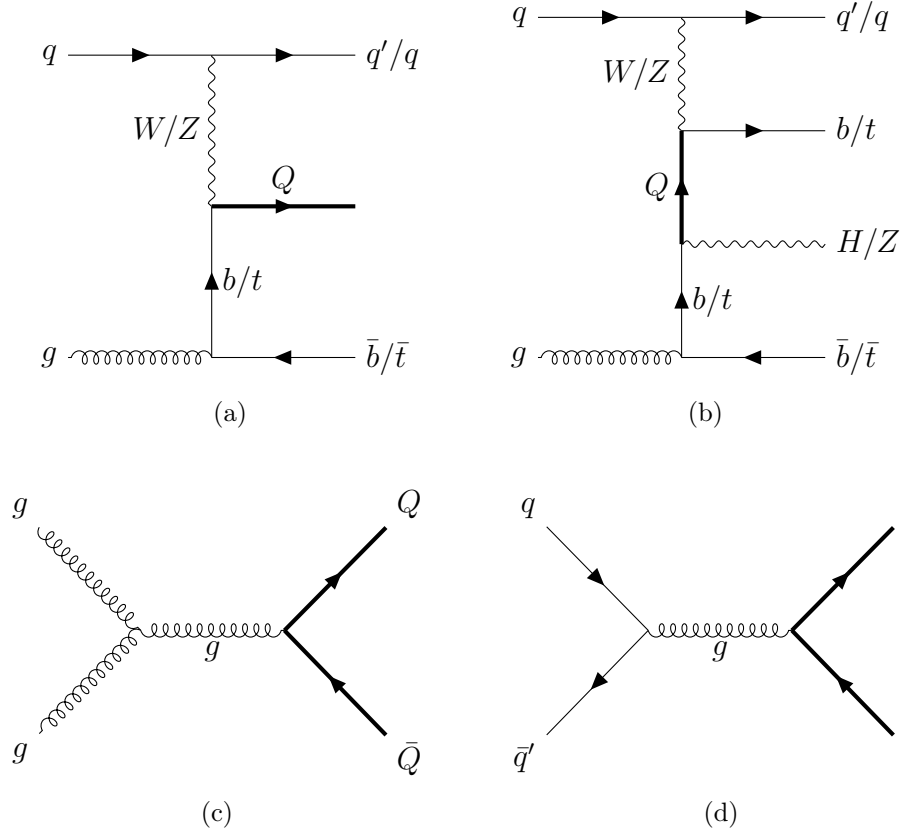


Figure 1: Representative VLQ production topologies: single production in panels (a) and (b), and pair production in panels (c) and (d).

The VLQBounds approach combines

1. experimental upper limits on final-state signatures,
2. theoretical predictions for pair- and single-production rates, and
3. BRs into the experimentally relevant decay modes.

For a given model point, the code maps the user input onto the appropriate experimental variables, evaluates the relevant theory prediction, and compares it with the published observed and expected limits. This allows exclusion regions to be derived without a detector-level reanalysis.

LHC searches for VLQs cover a broad range of theoretical scenarios, from simplified models in which a single VLQ decays into a fixed SM final state to complete EW multiplets such as singlets, doublets, or triplets. Current analyses exclude VLQ masses up to the TeV scale, depending on the assumed decay pattern and production mechanism. The limits arise from searches involving  $W$ ,  $Z$ , or Higgs bosons in association with heavy-flavour quarks as well as multilepton and boosted-object analyses designed to enhance sensitivity to heavy resonances.

To facilitate reinterpretation, the relevant searches are implemented in the VLQBounds framework. The included analyses are summarised in Tables 2-7. For each search, the relevant theoretical prediction  $\sigma_{\text{theo}}$  is compared with the corresponding observed and expected limits,  $\sigma_{\text{obs}}$  and  $\sigma_{\text{exp}}$ , using the native variables of the experimental publication.

#### 4. Experimental Datasets

The implemented dataset collection includes ATLAS and CMS searches relevant to pair and single production of VLQs at the LHC. The searches cover top partners  $T$ , bottom partners  $B$ , and the exotic partners  $X$  and  $Y$ , with decay topologies involving  $W$ ,  $Z$ , and the SM Higgs boson in association with heavy-flavour quarks. The implementation is organised through machine-readable JSON inputs supplemented by metadata specifying the experiment, centre-of-mass energy, integrated luminosity, process, decay topology, lepton multiplicity, and native limit representation.

Because published limits are provided at discrete mass, coupling, and/or width values, interpolation is required to evaluate arbitrary model points. One-dimensional curves are treated by shape-preserving or linear interpolation in the published mass variable. Two-dimensional surfaces are interpolated in the native plane, such as  $(m_Q, \kappa)$  or  $(m_Q, \Gamma_Q/m_Q)$ . The framework does not extrapolate beyond the published kinematic coverage, rather, points outside the available domain are flagged.

#### 4.1. Methodology

*Signal Hypotheses.* We consider both QCD pair production,

$$pp \rightarrow Q\bar{Q},$$

and EW single production,

$$pp \rightarrow Qq,$$

where  $Q \in \{T, B, X, Y\}$  and  $q$  denotes a SM quark. Pair production depends predominantly on  $m_Q$ , while single production depends on  $m_Q$  and a coupling-like parameter expressed as  $s_{L/R}$ ,  $\kappa$ , or  $\Gamma_Q/m_Q$ .

*Test Statistics and Decision Rule.* For each experimental channel  $I$  with observed and expected 95% CL upper limits  $\sigma_{\text{obs}}^I$  and  $\sigma_{\text{exp}}^I$ , we compute

$$r_{\text{obs}}^I = \frac{\sigma_{\text{theo}}^I}{\sigma_{\text{obs}}^I}, \quad r_{\text{exp}}^I = \frac{\sigma_{\text{theo}}^I}{\sigma_{\text{exp}}^I}, \quad (3)$$

where  $\sigma_{\text{theo}}^I$  is the corresponding theory prediction. The most sensitive channel is selected by maximising  $r_{\text{exp}}^I$ , with ties resolved through  $r_{\text{obs}}^I$ . The point is excluded at 95% CL if the observed ratio of the selected channel satisfies  $r_{\text{obs}} \geq 1$ . This avoids combining statistically independent experimental analyses without the full likelihood information.

VLQ	ATLAS	$\sqrt{s}$	Luminosity	Decay	Lepton multiplicity
<i>T</i> Singlet	<a href="#">32</a>	13 TeV	36.1 fb <sup>-1</sup>	$Z(\nu\nu)t$	1 $\ell$
	<a href="#">33</a>	13 TeV	36.1 fb <sup>-1</sup>	$W^\pm b$	0 $\ell$
	<a href="#">34</a>	13 TeV	36.1 fb <sup>-1</sup>	Inclusive	2 $\ell$ SS
	<a href="#">35</a>	13 TeV	36.1 fb <sup>-1</sup>	$W(\ell\nu)b$	1 $\ell$
	<a href="#">36</a>	13 TeV	139 fb <sup>-1</sup>	$H(bb)t$	0 $\ell$
	<a href="#">37</a>	13 TeV	139 fb <sup>-1</sup>	Inclusive	1 $\ell$
	<a href="#">38</a>	13 TeV	36.1 fb <sup>-1</sup>	$Ht, Zt$	1 $\ell$
	<a href="#">39</a>	13 TeV	139 fb <sup>-1</sup>	$Z(\ell\ell)t$	2 $\ell$ OS, 3 $\ell$
	<a href="#">40</a>	13 TeV	139 fb <sup>-1</sup>	$H(b\bar{b})t, Z(qq)t$	1 $\ell$
	<a href="#">41</a>	13 TeV	139 fb <sup>-1</sup>	$Z(\ell\ell)t$	2 $\ell$ OS, 3 $\ell$
	<a href="#">42</a>	13 TeV	140 fb <sup>-1</sup>	$Z(\nu\nu)t$	0 $\ell$
	<a href="#">43</a>	13 TeV	140 fb <sup>-1</sup>	Inclusive	1 $\ell$
	<a href="#">44</a>	13 TeV	36.1 fb <sup>-1</sup>	$Z(\nu\nu)t$	0 $\ell, 1\ell$
	<a href="#">45</a>	13 TeV	3.2 fb <sup>-1</sup>	$W^\pm b$	1 $\ell$
	<a href="#">46</a>	13 TeV	13.2 fb <sup>-1</sup>	Inclusive	1 $\ell, 0\ell$
	<a href="#">47</a>	13 TeV	3.2 fb <sup>-1</sup>	Inclusive	2 $\ell$ SS, 3 $\ell$
	<a href="#">48</a>	8 TeV	20.3 fb <sup>-1</sup>	$W(\ell\nu)b$	1 $\ell$
	<a href="#">49</a>	8 TeV	20.3 fb <sup>-1</sup>	$Zt$	2 $\ell$ OS, 3 $\ell$
	<a href="#">50</a>	8 TeV	20.3 fb <sup>-1</sup>	Inclusive	1 $\ell$
	<a href="#">51</a>	8 TeV	20.3 fb <sup>-1</sup>	Inclusive	2 $\ell$ SS
	<a href="#">52</a>	13 TeV	36.1 fb <sup>-1</sup>	Inclusive	1 $\ell, 2\ell$ SS, 3 $\ell$
	<a href="#">53</a>	8 TeV	20.3 fb <sup>-1</sup>	Inclusive	1 $\ell$
	<a href="#">54</a>	13 TeV	139 fb <sup>-1</sup>	$Ht, Zt$	0 $\ell, 1\ell, \geq 2\ell$
	<a href="#">55</a>	13 TeV	36.1 fb <sup>-1</sup>	$Zt$	2 $\ell$ OS
	<a href="#">56</a>	13 TeV	139 fb <sup>-1</sup>	$W^\pm b$	0 $\ell$
	<a href="#">57</a>	13 TeV	140 fb <sup>-1</sup>	$W(\ell\nu)b$	1 $\ell$
	<a href="#">58</a>	13 TeV	140 fb <sup>-1</sup>	$W(\ell\nu)b$	1 $\ell$
	<i>T</i> Doublet	<a href="#">32</a>	13 TeV	36.1 fb <sup>-1</sup>	$Z(\nu\nu)t$
<a href="#">37</a>		13 TeV	139 fb <sup>-1</sup>	Inclusive	1 $\ell$
<a href="#">38</a>		13 TeV	36.1 fb <sup>-1</sup>	$Ht, Zt$	1 $\ell$
<a href="#">39</a>		13 TeV	139 fb <sup>-1</sup>	$Z(\ell\ell)t$	2 $\ell$ OS, 3 $\ell$
<a href="#">40</a>		13 TeV	139 fb <sup>-1</sup>	$H(b\bar{b})t, Z(qq)t$	1 $\ell$
<a href="#">41</a>		13 TeV	139 fb <sup>-1</sup>	$Z(\ell\ell)t$	2 $\ell$ OS, 3 $\ell$
<a href="#">46</a>		13 TeV	13.2 fb <sup>-1</sup>	Inclusive	1 $\ell$
<a href="#">52</a>		13 TeV	36.1 fb <sup>-1</sup>	Inclusive	1 $\ell, 2\ell$ SS, 3 $\ell$
<a href="#">49</a>		8 TeV	20.3 fb <sup>-1</sup>	$Zt$	2 $\ell$ OS, 3 $\ell$
<a href="#">50</a>		8 TeV	20.3 fb <sup>-1</sup>	Inclusive	1 $\ell$
<a href="#">54</a>	13 TeV	139 fb <sup>-1</sup>	$Ht, Zt$	0 $\ell, 1\ell, \geq 2\ell$	
BR=100%	<a href="#">32</a>	13 TeV	36.1 fb <sup>-1</sup>	$Z(\nu\nu)t$	1 $\ell$
	<a href="#">33</a>	13 TeV	36.1 fb <sup>-1</sup>	$W^\pm b$	0 $\ell$
	<a href="#">59</a>	13 TeV	36.1 fb <sup>-1</sup>	Inclusive	0 $\ell$
	<a href="#">37</a>	13 TeV	139 fb <sup>-1</sup>	Inclusive	1 $\ell$
	<a href="#">39</a>	13 TeV	139 fb <sup>-1</sup>	$Z(\ell\ell)t$	2 $\ell$ OS, 3 $\ell$
	<a href="#">60</a>	13 TeV	3.2 fb <sup>-1</sup>	Inclusive	1 $\ell$
	<a href="#">45</a>	13 TeV	3.2 fb <sup>-1</sup>	$W^\pm(\ell\nu)b$	1 $\ell$
	<a href="#">46</a>	13 TeV	13.2 fb <sup>-1</sup>	Inclusive	1 $\ell, 0\ell$
	<a href="#">61</a>	7 TeV	4.7 fb <sup>-1</sup>	$W^\pm b$	0 $\ell$
	<a href="#">50</a>	8 TeV	20.3 fb <sup>-1</sup>	Inclusive	1 $\ell$
	<a href="#">62</a>	7 TeV	1.04 fb <sup>-1</sup>	$W^\pm b$	1 $\ell$
	<a href="#">43</a>	13 TeV	140 fb <sup>-1</sup>	Inclusive	1 $\ell$
	<a href="#">55</a>	13 TeV	36.1 fb <sup>-1</sup>	$Zt$	2 $\ell$ OS

Table 2: Summary of ATLAS searches for the vector-like top partner. Here,  $\ell = e, \mu$  and OS(SS) refers to the Opposite(Same) Sign case.

VLQ	ATLAS	$\sqrt{s}$	Luminosity	Decay	Lepton multiplicity
<i>B</i> Singlet	<a href="#">33</a>	13 TeV	36.1 fb <sup>-1</sup>	$W^{\pm}t$	0 $\ell$
	<a href="#">34</a>	13 TeV	36.1 fb <sup>-1</sup>	Inclusive	2 $\ell$ SS
	<a href="#">37</a>	13 TeV	139 fb <sup>-1</sup>	Inclusive	1 $\ell$
	<a href="#">39</a>	13 TeV	139 fb <sup>-1</sup>	$Z(\ell\ell)b$	2 $\ell$ OS, 3 $\ell$
	<a href="#">47</a>	13 TeV	3.2 fb <sup>-1</sup>	Inclusive	2 $\ell$ SS, 3 $\ell$
	<a href="#">52</a>	13 TeV	36.1 fb <sup>-1</sup>	Inclusive	1 $\ell$ , 2 $\ell$ SS, 3 $\ell$
	<a href="#">49</a>	8 TeV	20.3 fb <sup>-1</sup>	$Zb$	2 $\ell$ OS, 3 $\ell$
	<a href="#">50</a>	8 TeV	20.3 fb <sup>-1</sup>	Inclusive	1 $\ell$
	<a href="#">51</a>	8 TeV	20.3 fb <sup>-1</sup>	Inclusive	2 $\ell$ SS
	<a href="#">63</a>	13 TeV	139 fb <sup>-1</sup>	$bH(bb)$	0 $\ell$
	<a href="#">64</a>	13 TeV	36.1 fb <sup>-1</sup>	$W^{\pm}t$	1 $\ell$
<a href="#">53</a>	8 TeV	20.3 fb <sup>-1</sup>	Inclusive	1 $\ell$	
<i>B</i> Doublet	<a href="#">59</a>	13 TeV	36.1 fb <sup>-1</sup>	Inclusive	0 $\ell$
	<a href="#">35</a>	13 TeV	36.1 fb <sup>-1</sup>	$W^{\pm}b\ell\nu$	1 $\ell$
	<a href="#">37</a>	13 TeV	139 fb <sup>-1</sup>	Inclusive	1 $\ell$
	<a href="#">39</a>	13 TeV	139 fb <sup>-1</sup>	$Z(\ell\ell)b$	2 $\ell$ OS, 3 $\ell$
	<a href="#">52</a>	13 TeV	36.1 fb <sup>-1</sup>	Inclusive	1 $\ell$ , 2 $\ell$ SS, 3 $\ell$
	<a href="#">49</a>	8 TeV	20.3 fb <sup>-1</sup>	$Zb$	2 $\ell$ OS, 3 $\ell$
<a href="#">63</a>	13 TeV	139 fb <sup>-1</sup>	$bH(bb)$	0 $\ell$	
BR=100%	<a href="#">33</a>	13 TeV	36.1 fb <sup>-1</sup>	$W^{\pm}t$	0 $\ell$
	<a href="#">35</a>	13 TeV	36.1 fb <sup>-1</sup>	$Z(\ell\ell)b$	2 $\ell$ OS, $\geq$ 3 $\ell$
	<a href="#">59</a>	13 TeV	36.1 fb <sup>-1</sup>	Inclusive	0 $\ell$
	<a href="#">37</a>	13 TeV	139 fb <sup>-1</sup>	Inclusive	1 $\ell$
	<a href="#">39</a>	13 TeV	139 fb <sup>-1</sup>	$Z(\ell\ell)b$	2 $\ell$ OS, 3 $\ell$
	<a href="#">64</a>	13 TeV	36.1 fb <sup>-1</sup>	$W^{\pm}t$	1 $\ell$
	<a href="#">65</a>	8 TeV	20.3 fb <sup>-1</sup>	$W^{\pm}t$	1 $\ell$ , 2 $\ell$
	<a href="#">50</a>	8 TeV	20.3 fb <sup>-1</sup>	Inclusive	1 $\ell$

Table 3: Summary of ATLAS searches for the vector-like bottom partner. Here,  $\ell = e, \mu$  and OS(SS) refers to the Opposite(Same) Sign case.

VLQ	ATLAS	$\sqrt{s}$	Luminosity	Decay	Lepton multiplicity
$X$	<a href="#">33</a>	13 TeV	$36.1 \text{ fb}^{-1}$	$W^{\pm}t$	$0\ell$
	<a href="#">34</a>	13 TeV	$36.1 \text{ fb}^{-1}$	Inclusive	$2\ell \text{ SS}$
	<a href="#">64</a>	13 TeV	$36.1 \text{ fb}^{-1}$	$W^{\pm}t$	$1\ell$
	<a href="#">34</a>	13 TeV	$36.1 \text{ fb}^{-1}$	$W^{\pm}t$	$2\ell \text{ SS}$
	<a href="#">47</a>	13 TeV	$3.2 \text{ fb}^{-1}$	Inclusive	$2\ell \text{ SS}, 3\ell$
	<a href="#">51</a>	8 TeV	$20.3 \text{ fb}^{-1}$	Inclusive	$2\ell \text{ SS}$
$Y$	<a href="#">53</a>	8 TeV	$20.3 \text{ fb}^{-1}$	Inclusive	$1\ell$
	<a href="#">33</a>	13 TeV	$36.1 \text{ fb}^{-1}$	$W^{\pm}b$	$0\ell$
	<a href="#">43</a>	13 TeV	$140 \text{ fb}^{-1}$	Inclusive	$1\ell$
Doublet $X$	<a href="#">48</a>	8 TeV	$20.3 \text{ fb}^{-1}$	$W^{\pm}(\ell\nu)b$	$1\ell$
	<a href="#">37</a>	13 TeV	$139 \text{ fb}^{-1}$	$W^{\pm}t$	$1\ell$
Doublet $Y$	<a href="#">48</a>	8 TeV	$20.3 \text{ fb}^{-1}$	$W(\ell\nu)b$	$1\ell$
	<a href="#">45</a>	13 TeV	$3.2 \text{ fb}^{-1}$	$W^{\pm}b$	$1\ell$
	<a href="#">35</a>	13 TeV	$36.1 \text{ fb}^{-1}$	$W(\ell\nu)b$	$1\ell$
	<a href="#">45</a>	13 TeV	$3.2 \text{ fb}^{-1}$	$W(\ell\nu)b$	$1\ell$
	<a href="#">56</a>	13 TeV	$139 \text{ fb}^{-1}$	$W^{\pm}b$	$0\ell$
Triplet $Y$	<a href="#">35</a>	13 TeV	$36.1 \text{ fb}^{-1}$	$W^{\pm}(\ell\nu)b$	$1\ell$
	<a href="#">57</a>	13 TeV	$140 \text{ fb}^{-1}$	$W(\ell\nu)b$	$1\ell$

Table 4: Summary of ATLAS searches for the exotic VLQs  $X$  and  $Y$ . Here,  $\ell = e, \mu$  and OS(SS) refers to the Opposite(Same) Sign case.

VLQ	CMS	$\sqrt{s}$	Luminosity	Decay	Lepton multiplicity
<i>T</i> Singlet	[66]	13 TeV	137 fb <sup>-1</sup>	$Z(\nu\nu)t$	0 $\ell$
	[67]	13 TeV	2.3 fb <sup>-1</sup>	$H(bb)t$	0 $\ell$
	[68]	13 TeV	2.3 fb <sup>-1</sup>	$H(bb)t$	0 $\ell$
	[69]	13 TeV	2.6 fb <sup>-1</sup>	Inclusive	1 $\ell$
	[70]	13 TeV	138 fb <sup>-1</sup>	$H(\gamma\gamma)t$	0 $\ell, 1\ell$
	[71]	13 TeV	138 fb <sup>-1</sup>	$Ht, Zt$	0 $\ell$
	[72]	13 TeV	35.9 fb <sup>-1</sup>	$Ht, Zt$	0 $\ell$
	[73]	13 TeV	35.9 fb <sup>-1</sup>	$Z(\ell\ell)t$	2 $\ell$ OS
	[74]	13 TeV	2.3 fb <sup>-1</sup>	Inclusive	1 $\ell$
	[75]	8 TeV	19.5 fb <sup>-1</sup>	Inclusive	1 $\ell$
	[76]	7 TeV	5.0 fb <sup>-1</sup>	$W^\pm(\ell\nu)b$	1 $\ell$
	[77]	13 TeV	35.9 fb <sup>-1</sup>	Inclusive	1 $\ell, 2\ell$ SS, 3 $\ell$
	[78]	13 TeV	138 fb <sup>-1</sup>	Inclusive	1 $\ell, 2\ell$ SS, 3 $\ell$
	[79]	13 TeV	2.3 fb <sup>-1</sup>	$Zt$	0 $\ell$
	[80]	13 TeV	138 fb <sup>-1</sup>	$Ht$	1 $\ell$
[81]	13 TeV	138 fb <sup>-1</sup>	$W^\pm b, Zt, Ht$	1 $\ell, 2\ell$ SS, $\geq 3\ell$	
<i>T</i> Doublet	[67]	13 TeV	2.3 fb <sup>-1</sup>	$H(bb)t$	0 $\ell$
	[77]	13 TeV	35.9 fb <sup>-1</sup>	Inclusive	1 $\ell, 2\ell$ SS, 3 $\ell$
	[68]	13 TeV	2.3 fb <sup>-1</sup>	$H(bb)t$	0 $\ell$
	[82]	13 TeV	35.9 fb <sup>-1</sup>	$Z(\ell\ell)t$	2 $\ell$ OS
	[69]	13 TeV	2.6 fb <sup>-1</sup>	Inclusive	1 $\ell$
	[79]	13 TeV	2.3 fb <sup>-1</sup>	$Zt$	0 $\ell$
	[73]	13 TeV	35.9 fb <sup>-1</sup>	$Z(\ell\ell)t$	2 $\ell$ OS
	[72]	13 TeV	35.9 fb <sup>-1</sup>	$Ht, Zt$	0 $\ell$
	[78]	13 TeV	138 fb <sup>-1</sup>	Inclusive	1 $\ell, 2\ell$ SS, 3 $\ell$
[81]	13 TeV	138 fb <sup>-1</sup>	$W^\pm b, Zt, Ht$	1 $\ell, 2\ell$ SS, $\geq 3\ell$	
BR=100%	[83]	13 TeV	2.3 fb <sup>-1</sup>	$W^\pm(\ell\nu)b$	1 $\ell$
	[82]	13 TeV	35.9 fb <sup>-1</sup>	$Z(\ell\ell)t$	2 $\ell$ OS
	[69]	13 TeV	2.6 fb <sup>-1</sup>	Inclusive	1 $\ell$
	[84]	13 TeV	35.8 fb <sup>-1</sup>	$W^\pm b$	1 $\ell$
	[85]	13 TeV	36.1 fb <sup>-1</sup>	Inclusive	0 $\ell$
	[86]	13 TeV	19.7 fb <sup>-1</sup>	Inclusive	1 $\ell, 2\ell$
	[87]	7 TeV	5.0 fb <sup>-1</sup>	$W^\pm b$	2 $\ell$
	[88]	8 TeV	19.7 fb <sup>-1</sup>	$H(bb)t$	0 $\ell$

Table 5: Summary of CMS searches for the vector-like top partner. Here,  $\ell = e, \mu$  and OS(SS) refers to the Opposite(Same) Sign case.

VLQ	CMS	$\sqrt{s}$	Luminosity	Decay	Lepton multiplicity
<i>B</i> Singlet	[69]	13 TeV	2.6 fb <sup>-1</sup>	Inclusive	1 $\ell$
	[77]	13 TeV	35.9 fb <sup>-1</sup>	Inclusive	1 $\ell$ , 2 $\ell$ SS, 3 $\ell$
	[78]	13 TeV	138 fb <sup>-1</sup>	Inclusive	1 $\ell$ , 2 $\ell$ SS, 3 $\ell$
	[79]	13 TeV	2.3 fb <sup>-1</sup>	<i>Zb</i>	0 $\ell$
	[89]	13 TeV	35.9 fb <sup>-1</sup>	<i>H(bb)b</i>	0 $\ell$
	[90]	13 TeV	138 fb <sup>-1</sup>	<i>W<sup>±</sup>t</i>	0 $\ell$
	[81]	13 TeV	138 fb <sup>-1</sup>	<i>Wt, Zb, Hb</i>	1 $\ell$ , 2 $\ell$ SS, $\geq$ 3 $\ell$
	[91]	13 TeV	138 fb <sup>-1</sup>	Inclusive	0 $\ell$ , 2 $\ell$ SS
<i>B</i> Doublet	[82]	13 TeV	35.9 fb <sup>-1</sup>	<i>Z(<math>\ell\ell</math>)b</i>	2 $\ell$ OS
	[69]	13 TeV	2.6 fb <sup>-1</sup>	Inclusive	1 $\ell$
	[77]	13 TeV	35.9 fb <sup>-1</sup>	Inclusive	1 $\ell$ , 2 $\ell$ SS, 3 $\ell$
	[78]	13 TeV	138 fb <sup>-1</sup>	Inclusive	1 $\ell$ , 2 $\ell$ SS, 3 $\ell$
	[89]	13 TeV	35.9 fb <sup>-1</sup>	<i>H(bb)b</i>	0 $\ell$
	[92]	13 TeV	138 fb <sup>-1</sup>	<i>Hb, Zb</i>	0 $\ell$
	[91]	13 TeV	138 fb <sup>-1</sup>	Inclusive	0 $\ell$ , 2 $\ell$ SS
	[79]	13 TeV	2.3 fb <sup>-1</sup>	<i>Zb</i>	0 $\ell$
BR=100%	[81]	13 TeV	138 fb <sup>-1</sup>	<i>Wt, Zb, Hb</i>	1 $\ell$ , 2 $\ell$ SS, $\geq$ 3 $\ell$
	[82]	13 TeV	35.9 fb <sup>-1</sup>	<i>Z(<math>\ell\ell</math>)b</i>	2 $\ell$ OS
	[85]	13 TeV	36.1 fb <sup>-1</sup>	Inclusive	0 $\ell$
	[92]	13 TeV	137 fb <sup>-1</sup>	<i>Hb, Zb</i>	0 $\ell$
	[91]	13 TeV	138 fb <sup>-1</sup>	Inclusive	0 $\ell$ , 2 $\ell$ SS
	[93]	8 TeV	19.7 fb <sup>-1</sup>	Inclusive	1 $\ell$ , 2 $\ell$ OS, $\geq$ 3 $\ell$
[94]	13 TeV	35.9 fb <sup>-1</sup>	<i>W<sup>±</sup>t</i>	1 $\ell$	

Table 6: Summary of CMS searches for the vector-like bottom partner. Here,  $\ell = e, \mu$  and OS(SS) refers to the Opposite(Same) Sign case.

VLQ	CMS	$\sqrt{s}$	Luminosity	Decay	Lepton multiplicity
BR=100% <i>X</i>	[94]	13 TeV	35.9 fb <sup>-1</sup>	<i>W<sup>±</sup>t</i>	1 $\ell$
	[95]	13 TeV	35.9 fb <sup>-1</sup>	<i>W<sup>±</sup>t</i>	1 $\ell$ , 2 $\ell$ SS
BR=100% <i>Y</i>	[83]	13 TeV	2.3 fb <sup>-1</sup>	<i>W<sup>±</sup>(<math>\ell\nu</math>)b</i>	1 $\ell$
	[84]	13 TeV	35.8 fb <sup>-1</sup>	<i>W<sup>±</sup>b</i>	1 $\ell$
Triplet <i>Y</i>	[91]	13 TeV	138 fb <sup>-1</sup>	Inclusive	0 $\ell$ , 2 $\ell$ SS

Table 7: Summary of CMS searches for the exotic VLQs *X* and *Y*. Here,  $\ell = e, \mu$  and OS(SS) refers to the Opposite(Same) Sign case.

*Interpolation and Extrapolation Policy.* All experimental inputs are represented in their native published variables. VLQBounds interpolates only inside the covered domain. No extrapolation is performed outside the available grid or curve range.

*Coupling-space Comparisons.* When an analysis publishes limits directly on  $\kappa(m_Q)$ , user inputs provided in terms of  $s_{L/R}$  or  $\Gamma_Q/m_Q$  are translated into  $\kappa$  using Table 1. The comparison is then performed directly in the  $(m_Q, \kappa)$  plane.

## 5. Software Architecture

The current VLQBounds codebase follows a modern Python package layout and separates model definitions, physics utilities, experimental-data access, inference logic, and validation plotting. This structure is essential for reproducibility, because the validation figures and scan outputs are generated directly from the same internal data files and model classes used by the exclusion engine. The public source tree is intended to be distributed through GitHub at <https://github.com/MBKBD/VLQBounds>. In the final submission package, this repository will provide the tagged release, the machine-readable tables used by the code, and the example scripts employed to reproduce the validation plots and benchmark scans discussed in this work.

### 5.1. Design Goals

The main design goals are:

- *Data-driven evaluation:* experimental limits and theory tables are stored as machine-readable JSON inputs and loaded through the internal repository layer.
- *Uniform model interface:* all supported VLQ representations expose common setters for mass, mixing, coupling, and width inputs.
- *Native-limit interpretation:* cross-section limits, coupling limits, and width-scan limits are treated in their published variables.
- *Transparent reporting:* the code returns the exclusion verdict, observed and expected ratios, dominant channel, process, experiment, luminosity, energy, and reference label.

- *Direct validation plotting*: official-style validation plots can be generated directly from VLQBounds, without embedding external numerical arrays in the user script.

## 5.2. Package Map

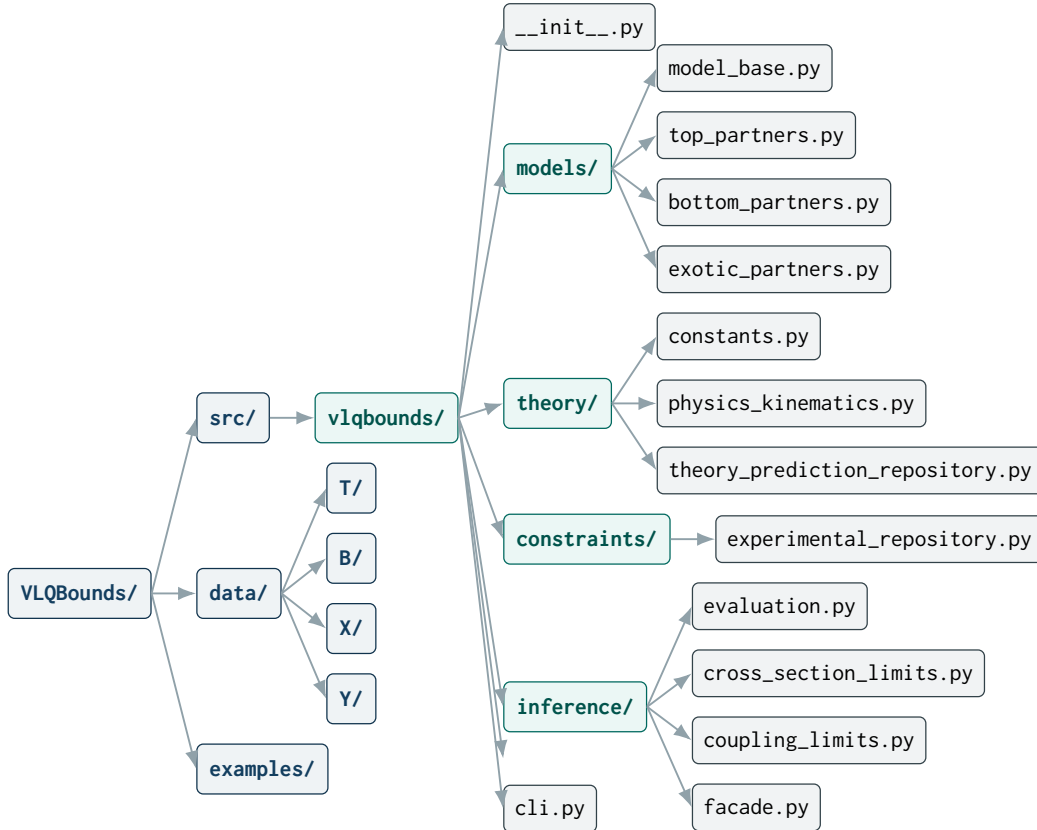


Figure 2: Layout of the VLQBounds repository.

Figure 2 summarises the current package organisation. The installable package is located under `src/vlqbounds`. The `models` subpackage contains the VLQ classes, `theory` stores physics utilities and theory tables, `constraints` provides access to experimental repositories, `inference` contains the public VLQBounds facade, and `validation` contains the internal plotting tools for mass-width and mass-coupling validation figures.

### 5.3. Model Classes and Public Setters

The current model layer is based on the following classes:

Model class hierarchy
VectorLikeModelBase
TopPartnerSinglet
TopPartnerDoublet
TopPartnerPure
BottomPartnerSinglet
BottomPartnerDoublet
BottomPartnerPure
XPartnerDoublet
YPartnerDoublet
YPartnerTriplet

Each model class is called through the public VLQBounds facade. The supported parameter-setter methods are summarised in Table 8. Each call requires a mass and one companion parameter: a mixing angle, an effective coupling, or a relative width.

Setter method	Mass keyword	Accepted companion keywords
singletT_params	mT	s_l, k_T, w_m
doubletT_XT_params	mT	s_r, k_T, w_m
doubletT_TB_params	mT	s_u_r, k_T, w_m
singletB_params	mB	s_l, k_B, w_m
doubletB_BY_params	mB	s_r, k_B, w_m
doubletB_TB_params	mB	s_d_r, k_B, w_m
doubletX_XT_params	mX	s_r, k_X, w_m
doubletY_BY_params	mY	s_r, k_Y, w_m
tripletY_TBY_params	mY	s_d_l, k_Y, w_m

Table 8: Public parameter-setter methods exposed by the VLQBounds facade.

#### 5.4. Execution Pipeline

##### Deterministic decision flow

1. **Model construction.** The user instantiates a model class from `vlqbounds.models` and passes it to `VLQBounds`.
2. **Analysis preparation.** The method `prepare_analysis()` loads cross-section inputs, coupling-limit tables, and the internal dictionaries required for the active VLQ species and representation.
3. **Parameter assignment.** The user calls a typed setter such as `singletT_params(mT=..., s_l=...)`, `doubletB_BY_params(mB=..., w_m=...)`, or `doubletT_TB_params(mT=..., k_T=...)`.
4. **Theory evaluation.** The active model computes masses, mixing angles, effective couplings, widths, BRs, and theory cross-sections.
5. **Limit interpolation.** The inference layer interpolates the relevant observed and expected experimental limits in the native published variables.
6. **Decision.** Channel-wise ratios are built using Eq. (3). The most sensitive channel is selected and the exclusion verdict is stored.
7. **Reporting.** Results are printed to the terminal, appended to the internal `pandas DataFrame`, and can be exported for scans or plotting.

#### 5.5. Public API

A minimal single-point evaluation has the form:

```

1  from vlqbounds.models import TopPartnerSinglet
2  from vlqbounds.inference import VLQBounds
3
4  bounds = VLQBounds(TopPartnerSinglet())
5  bounds.prepare_analysis()
6
7  bounds.singletT_params(mT=1500.0, s_l=0.10)
8  bounds.check_against_xs_and_coupling_limits()
9
10 bounds.print_result()
11 print(bounds.df.tail(1).T)

```

Listing 1: Single-point evaluation with the current VLQBounds facade.

The same interface works for other species and representations:

```

1  from vlqbounds.models import (
2  TopPartnerDoublet,
3  BottomPartnerDoublet,
4  XPartnerDoublet,
5  YPartnerTriplet,
6  )
7  from vlqbounds.inference import VLQBounds
8
9  # T doublet in the (T,B) representation
10 bounds_t = VLQBounds(TopPartnerDoublet())
11 bounds_t.prepare_analysis()
12 bounds_t.doubletT_TB_params(mT=1200.0, k_T=0.35)
13 bounds_t.check_against_xs_and_coupling_limits()
14
15 # B doublet in the (B,Y) representation
16 bounds_b = VLQBounds(BottomPartnerDoublet())
17 bounds_b.prepare_analysis()
18 bounds_b.doubletB_BY_params(mB=1000.0, w_m=0.05)
19 bounds_b.check_against_xs_and_coupling_limits()
20
21 # X doublet in the (X,T) representation
22 bounds_x = VLQBounds(XPartnerDoublet())
23 bounds_x.prepare_analysis()
24 bounds_x.doubletX_XT_params(mX=1300.0, s_r=0.20)
25 bounds_x.check_against_xs_and_coupling_limits()
26
27 # Y triplet in the (T,B,Y) representation

```

```

28 bounds_y = VLQBounds(YPartnerTriplet())
29 bounds_y.prepare_analysis()
30 bounds_y.tripletY_TBY_params(mY=1100.0, s_d_l=0.08)
31 bounds_y.check_against_xs_and_coupling_limits()

```

Listing 2: Representative calls for different VLQ representations.

### 5.6. Scan Interface

The example scripts distributed with the package use a small support module to run scans and save tables and plots. For example, a scan over the  $T$  singlet scenario is written as

```

1  import numpy as np
2
3  from vlqbounds.models import TopPartnerSinglet
4  from vlqbounds.inference import VLQBounds
5  from example_support import run_parameter_scan, save_scan_outputs
6
7
8  def configure(bounds, mass: float, mixing: float) -> None:
9  bounds.singletT_params(mT=mass, s_l=mixing)
10
11
12 def main() -> None:
13 model = TopPartnerSinglet()
14 bounds = VLQBounds(model)
15 bounds.prepare_analysis()
16
17 result_df = run_parameter_scan(
18 bounds=bounds,
19 parameter_callback=configure,
20 masses=np.arange(600, 2001, 200),
21 mixings=np.linspace(1e-5, 1.0, 10),
22 )
23
24 save_scan_outputs(
25 result_df,
26 output_stem="scan_t_singlet",
27 x_label=r"$m_T\, \mathrm{[GeV]}$",
28 title=r"$T\ \mathrm{Singlet}$",
29 xlim=(500, 2000),

```

```

30     ylim=(0.0, 0.5),
31     )
32
33
34     if __name__ == "__main__":
35         main()

```

Listing 3: Example scan script for the  $T$  singlet scenario.

Similarly, the  $B$  doublet in the  $(B, Y)$  representation is scanned as

```

1     import numpy as np
2
3     from vlqbounds.models import BottomPartnerDoublet
4     from vlqbounds.inference import VLQBounds
5     from example_support import run_parameter_scan, save_scan_outputs
6
7
8     def configure(bounds, mass: float, mixing: float) -> None:
9         bounds.doubletB_BY_params(mB=mass, s_r=mixing)
10
11
12     def main() -> None:
13         model = BottomPartnerDoublet()
14         bounds = VLQBounds(model)
15         bounds.prepare_analysis()
16
17         result_df = run_parameter_scan(
18             bounds=bounds,
19             parameter_callback=configure,
20             masses=np.arange(600, 2001, 200),
21             mixings=np.linspace(1e-5, 1.0, 10),
22         )
23
24         save_scan_outputs(
25             result_df,
26             output_stem="scan_b_doublet_by",
27             x_label=r"$m_{B\,}\mathrm{[GeV]}$",
28             title=r"$BY\ \mathrm{Doublet}$",
29         )
30
31
32     if __name__ == "__main__":

```

33

```
main()
```

Listing 4: Example scan script for the  $B$  doublet ( $B, Y$ ) scenario.

### 5.7. Internal Validation Plotting

The validation plotting tools are part of VLQBounds itself. The user script does not contain experimental or theory arrays; it only selects the internal limit key and output name.

For the CMS mass-width scan of Ref. [66], the validation figure is produced by

```

1  from vlqbounds.models import TopPartnerSinglet
2  from vlqbounds.inference import VLQBounds
3
4  bounds = VLQBounds(TopPartnerSinglet())
5  bounds.prepare_analysis()
6
7  surface, boundary = bounds.plot_width_scan_limit(
8  limit_key="cms_2201_02227_t_singlet_tzbq",
9  output_stem="validation_cms_2201_02227_t_singlet",
10 )

```

Listing 5: Internal CMS mass-width validation plot generated directly from VLQBounds.

For the ATLAS mass-coupling plot associated with Fig. 9 of Ref. [36], the internal coupling-limit plotter is called as

```

1   from vlqbounds.models import TopPartnerSinglet
2   from vlqbounds.inference import VLQBounds
3
4   bounds = VLQBounds(TopPartnerSinglet())
5   bounds.prepare_analysis()
6
7   curves = bounds.plot_coupling_limit_figure(
8   limit_key="atlas_2201_07045_fig9_t_singlet_ht",
9   output_stem="validation_atlas_2201_07045_fig9_t_singlet_ht",
10  use_tex=False,
11  debug=True,
12  )

```

Listing 6: Internal ATLAS mass-coupling validation plot generated directly from VLQBounds.

The validation tools read the relevant internal JSON files, reconstruct the observed and expected curves, and save the corresponding numerical outputs and figures. In this way, validation plots and scan plots are produced within the same package workflow.

### 5.8. *Command-line Usage*

After editable installation,

```

1 python -m pip install -e .
2 python examples/validation.py
3 python examples/scan_t_singlet.py

```

Listing 7: Editable installation and example execution.

## 6. Validation

VLQBounds retrieves the theoretical predictions and experimental limits directly from the machine-readable files included in the repository. For a given point, specified by the VLQ mass and either a coupling-like input or a relative width  $\Gamma_Q/m_Q$ , the framework evaluates the corresponding theory cross-section, interpolates the experimental upper limit, and constructs the sensitivity ratios of Eq. (3).

The CMS validation shown in Fig. 3 uses the published width slices  $\Gamma_T/m_T = 5\%$ ,  $10\%$ ,  $20\%$ , and  $30\%$  for the singlet  $T$  search in the  $tZbq$  final state [66]. The internal validation routine performs a structured interpolation: shape-preserving interpolation in mass within each published width slice, followed by interpolation in width. The red curve is defined by  $r_{\text{obs}} = 1$ , with the excluded region lying on the low-mass side of the contour.

Figure 4 shows the corresponding coupling-limit validation for the ATLAS analysis of Ref. [36]. In this case, VLQBounds reconstructs the observed and expected limits in the  $(m_T, \kappa_T)$  plane from the internal digitised data files. The same interface also overlays reference curves corresponding to fixed values of  $\Gamma_T/m_T$ , computed from the active `TopPartnerSinglet` model.

These validation examples test both the numerical interpolation and the internal mapping between user-level input parameters and the native variables used by the experimental searches. They also provide direct regression tests for the plotting layer, since the figures are generated using the same data repository and model interface used by the exclusion engine.

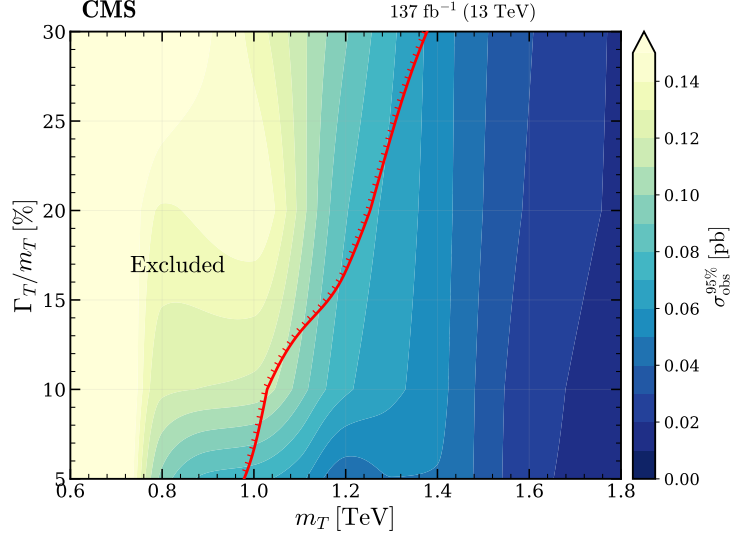


Figure 3: Observed 95% CL upper limit on  $\sigma(pp \rightarrow T b q \rightarrow t Z b q)$  in the  $(m_T, \Gamma_T/m_T)$  plane.

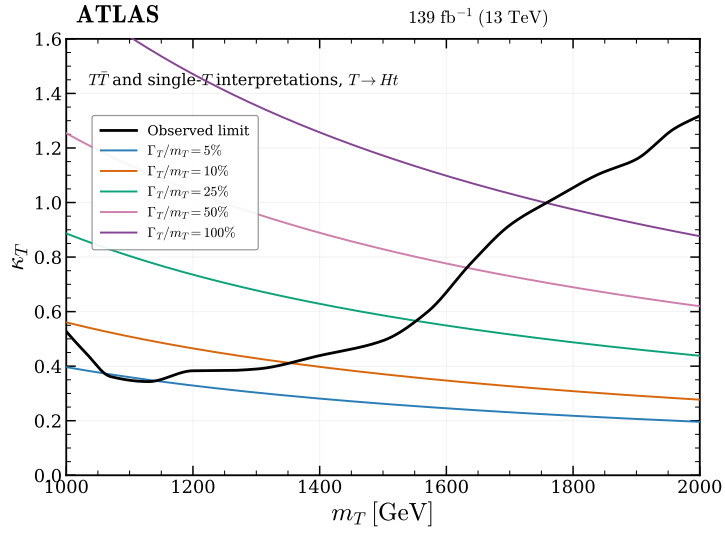


Figure 4: Observed and expected upper limits on the effective coupling  $\kappa_T$  as a function of the vector-like top mass.

## 7. Representative Results

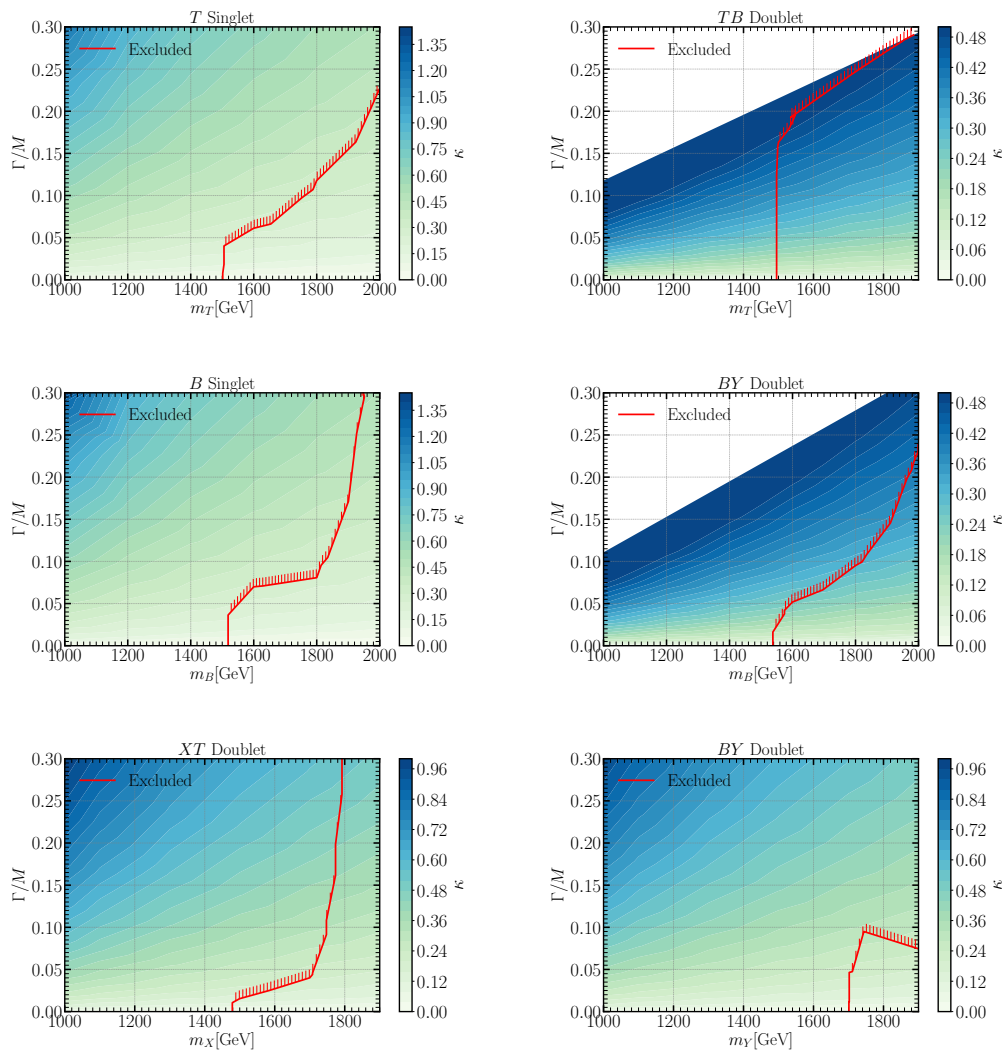


Figure 5: Observed 95% CL exclusion contours for six representative VLQ benchmark scenarios produced with VLQBounds.

We illustrate the workflow using six representative benchmark scenarios. For each scenario, the scan is performed in the  $(m_Q, \Gamma_Q/m_Q)$  plane. The colour map reports the corresponding effective coupling  $\kappa$ , while the red contour denotes the observed 95% CL exclusion boundary after selecting the

most sensitive analysis at each parameter point.

A typical structured output produced by VLQBounds is shown in Listing 8. The output records the model definition, the input parameters, derived quantities, the exclusion verdict, the most sensitive channel, and the metadata needed for reproducibility.

```
1  {
2    "scenario": {
3      "model": "TopPartnerSinglet",
4      "input": {
5        "mass_GeV": 1200.0,
6        "s_left": 0.4003
7      },
8      "derived": {
9        "width_over_mass": 0.1397,
10       "effective_kappa": 0.5661,
11       "br_Wb": 0.501,
12       "br_Zt": 0.249,
13       "br_Ht": 0.250
14     }
15   },
16   "result": {
17     "decision": "Excluded",
18     "result_flag": 0,
19     "observed_ratio": 5.00,
20     "expected_ratio": 4.42,
21     "dominant_channel": 45
22   },
23   "driving_analysis": {
24     "description": "See manifest metadata for the full
25       experimental record",
26     "note": "Most sensitive channel selected through expected
27       sensitivity."
28   },
29   "metadata": {
30     "vlqbounds_version": "0.1",
31     "generated_by": "VLQBounds runtime",
32     "data_format": "JSON"
33   }
34 }
```

Listing 8: Illustrative structured output produced by VLQBounds.

Figure 5 shows a common qualitative pattern. At small relative widths, exclusions are dominated by QCD pair-production searches, producing near-vertical mass thresholds. As the width increases, and hence as the effective coupling grows, single-production channels become increasingly important and extend the sensitivity to larger masses. Differences between singlet and doublet scenarios arise from the representation-dependent mapping between the mixing angle and  $\kappa$ , as well as from changes in the BRs.

**Program summary** (*Comput. Phys. Commun.*)

**Program title:** VLQBounds

**Licensing provisions:** open source.

**Repository:** <https://github.com/MDBKD/VLQBounds>

**Programming language:** Python 3.10+; plotting based on matplotlib.

**Nature of problem:** determine whether a user-specified VLQ hypothesis is excluded at 95% CL by public ATLAS and CMS searches.

**Solution method:** JSON-based loading of experimental inputs; conversion between mixing, effective-coupling, and relative-width parameterisations; calculation of partial widths and branching ratios; interpolation of cross-section and coupling limits; identification of the most sensitive channel; and reporting of results in terminal and tabular form.

**Restrictions:** parameter points outside the published experimental coverage are flagged and are not extrapolated.

## 8. Conclusions

We have presented VLQBounds, a Python framework for confronting VLQ scenarios with public ATLAS and CMS searches. The code accepts minimal user input – the VLQ species and representation, the heavy mass, and one of  $s_{L/R}$ ,  $\kappa$ , or  $\Gamma_Q/m_Q$  – and maps this information onto the native parameterisation of the relevant experimental limits. It then computes the corresponding production and decay information, performs interpolation within the pub-

lished domains, identifies the most sensitive analysis, and returns a 95% CL exclusion verdict together with diagnostic observables.

The implementation is deliberately conservative. Experimental information is used only within the published kinematic coverage, with no extrapolation beyond available grids. At the same time, the code is designed for reproducibility and extensibility: all results are traceable to machine-readable internal data files, and validation plots are generated directly through the same package interface used for physical scans.

Although the present implementation already covers a broad set of public VLQ limits, the structure of VLQBounds naturally accommodates future extensions. A particularly important next step is the extension from the present SM+VLQ implementation to a 2HDM+VLQ framework, where exotic decay channels such as  $T \rightarrow Ht$ ,  $T \rightarrow At$ ,  $T \rightarrow H^+b$ ,  $B \rightarrow Hb$ ,  $B \rightarrow Ab$ ,  $B \rightarrow H^-t$ , together with the corresponding modes involving the exotic  $X$  and  $Y$  states, become central ingredients of the phenomenology [12–20, 22]. Further extensions include additional single-production channels, Run-3 and High-Luminosity LHC projections, and future lepton-collider setups.

## Acknowledgments

M. Boukidi acknowledges the support of Narodowe Centrum Nauki under OPUS grant no. 2023/49/B/ST2/03862. SM is supported in part through the NExT Institute and STFC CG ST/X000583/1.

## References

- [1] J. A. Aguilar-Saavedra, R. Benbrik, S. Heinemeyer, M. Pérez-Victoria, Handbook of vectorlike quarks: Mixing and single production, Phys. Rev. D 88 (9) (2013) 094010. [arXiv:1306.0572](#), [doi:10.1103/PhysRevD.88.094010](#).
- [2] M. Buchkremer, G. Cacciapaglia, A. Deandrea, L. Panizzi, Model Independent Framework for Searches of Top Partners, Nucl. Phys. B 876 (2013) 376–417. [arXiv:1305.4172](#), [doi:10.1016/j.nuclphysb.2013.08.010](#).

- [3] B. Fuks, H.-S. Shao, QCD next-to-leading-order predictions matched to parton showers for vector-like quark models, *Eur. Phys. J. C* 77 (2) (2017) 135. [arXiv:1610.04622](#), [doi:10.1140/epjc/s10052-017-4686-z](#).
- [4] J. M. Alves, G. C. Branco, A. L. Cherchiglia, C. C. Nishi, J. T. Penedo, P. M. F. Pereira, M. N. Rebelo, J. I. Silva-Marcos, Vector-like singlet quarks: A roadmap, *Phys. Rept.* 1057 (2024) 1–69. [arXiv:2304.10561](#), [doi:10.1016/j.physrep.2023.12.004](#).
- [5] K. Agashe, R. Contino, A. Pomarol, The Minimal composite Higgs model, *Nucl. Phys. B* 719 (2005) 165–187. [arXiv:hep-ph/0412089](#), [doi:10.1016/j.nuclphysb.2005.04.035](#).
- [6] R. Contino, L. Da Rold, A. Pomarol, Light custodians in natural composite Higgs models, *Phys. Rev. D* 75 (2007) 055014. [arXiv:hep-ph/0612048](#), [doi:10.1103/PhysRevD.75.055014](#).
- [7] N. Arkani-Hamed, A. G. Cohen, E. Katz, A. E. Nelson, The Littlest Higgs, *JHEP* 07 (2002) 034. [arXiv:hep-ph/0206021](#), [doi:10.1088/1126-6708/2002/07/034](#).
- [8] M. Schmaltz, D. Tucker-Smith, Little Higgs review, *Ann. Rev. Nucl. Part. Sci.* 55 (2005) 229–270. [arXiv:hep-ph/0502182](#), [doi:10.1146/annurev.nucl.55.090704.151502](#).
- [9] L. Randall, R. Sundrum, A Large mass hierarchy from a small extra dimension, *Phys. Rev. Lett.* 83 (1999) 3370–3373. [arXiv:hep-ph/9905221](#), [doi:10.1103/PhysRevLett.83.3370](#).
- [10] M. Carena, A. D. Medina, B. Panes, N. R. Shah, C. E. M. Wagner, Collider phenomenology of gauge-Higgs unification scenarios in warped extra dimensions, *Phys. Rev. D* 77 (2008) 076003. [arXiv:0712.0095](#), [doi:10.1103/PhysRevD.77.076003](#).
- [11] J. L. Hewett, T. G. Rizzo, Low-Energy Phenomenology of Superstring Inspired E(6) Models, *Phys. Rept.* 183 (1989) 193. [doi:10.1016/0370-1573\(89\)90071-9](#).

- [12] A. Arhrib, R. Benbrik, M. Boukidi, S. Moretti, Anatomy of vector-like bottom-quark models in the alignment limit of the 2-Higgs doublet model type-II, *Eur. Phys. J. C* 84 (10) (2024) 1008. [arXiv:2403.13021](#), [doi:10.1140/epjc/s10052-024-13390-5](#).
- [13] A. Arhrib, R. Benbrik, M. Boukidi, B. Manaut, S. Moretti, Anatomy of vector-like top-quark models in the alignment limit of the 2-Higgs Doublet Model Type-II, *Eur. Phys. J. C* 85 (1) (2025) 2. [arXiv:2401.16219](#), [doi:10.1140/epjc/s10052-024-13692-8](#).
- [14] A. Arhrib, R. Benbrik, M. Boukidi, S. Moretti, Large Hadron Collider Signatures of Exotic Vector-Like Quarks within the 2-Higgs Doublet Model Type-II (9 2024). [arXiv:2409.20104](#).
- [15] R. Benbrik, M. Boukidi, S. Moretti, Probing charged Higgs bosons in the two-Higgs-doublet model type II with vectorlike quarks, *Phys. Rev. D* 109 (5) (2024) 055016. [arXiv:2211.07259](#), [doi:10.1103/PhysRevD.109.055016](#).
- [16] H. Abouabid, A. Arhrib, R. Benbrik, M. Boukidi, J. E. Falaki, The oblique parameters in the 2HDM with vector-like quarks: confronting  $M_W$  CDF-II anomaly, *J. Phys. G* 51 (7) (2024) 075001. [arXiv:2302.07149](#), [doi:10.1088/1361-6471/ad3f34](#).
- [17] R. Benbrik, M. Boukidi, S. Moretti, Charged Higgs Boson Mass Bounds in 2HDM-II: Impact of Vector-Like Quarks, *PoS ICHEP2024* (2025) 083. [arXiv:2409.16054](#), [doi:10.22323/1.476.0083](#).
- [18] R. Benbrik, M. Berrouj, M. Boukidi, Investigation of charged Higgs bosons production from vectorlike T quark decays at  $e\gamma$  collider, *Phys. Rev. D* 111 (1) (2025) 015027. [arXiv:2408.15985](#), [doi:10.1103/PhysRevD.111.015027](#).
- [19] A. Arhrib, R. Benbrik, M. Berrouj, M. Boukidi, B. Manaut, Search for charged Higgs bosons through vectorlike top quark pair production at the LHC, *Phys. Rev. D* 111 (9) (2025) 095026. [arXiv:2407.01348](#), [doi:10.1103/PhysRevD.111.095026](#).

- [20] R. Benbrik, M. Berrouj, M. Boukidi, A. Habjia, E. Ghourmin, L. Rahili, Search for single production of vector-like top partner  $T \rightarrow H^+ b$  and  $H^\pm \rightarrow t b^-$  at the LHC Run-III, *Phys. Lett. B* 843 (2023) 138024. [doi:10.1016/j.physletb.2023.138024](https://doi.org/10.1016/j.physletb.2023.138024).
- [21] R. Dermíšek, E. Lunghi, S. Shin, Hunting for Vectorlike Quarks, *JHEP* 04 (2019) 019, [Erratum: *JHEP* 10, 058 (2020)]. [arXiv:1901.03709](https://arxiv.org/abs/1901.03709), [doi:10.1007/JHEP04\(2019\)019](https://doi.org/10.1007/JHEP04(2019)019).
- [22] R. Benbrik, M. Berrouj, M. Boukidi, K. Kahime, Exploring vector-like top quark pair production via charged Higgs decays in multi-b-jet and opposite-sign dilepton final state at the LHC, *Eur. Phys. J. C* 85 (5) (2025) 500. [doi:10.1140/epjc/s10052-025-14237-3](https://doi.org/10.1140/epjc/s10052-025-14237-3).
- [23] R. Benbrik, M. Boukidi, M. Ech-chaouy, S. Moretti, K. Salime, Q.-S. Yan, Vector-Like Quarks at the LHC: A unified perspective from ATLAS and CMS exclusion limits, *JHEP* 03 (2025) 020. [arXiv:2412.01761](https://arxiv.org/abs/2412.01761), [doi:10.1007/JHEP03\(2025\)020](https://doi.org/10.1007/JHEP03(2025)020).
- [24] A. Banerjee, E. Bergeaas Kuutmann, V. Ellajosyula, R. Enberg, G. Ferretti, L. Panizzi, Vector-like quarks: Status and new directions at the LHC, *SciPost Phys. Core* 7 (2024) 079. [arXiv:2406.09193](https://arxiv.org/abs/2406.09193), [doi:10.21468/SciPostPhysCore.7.4.079](https://doi.org/10.21468/SciPostPhysCore.7.4.079).
- [25] D. Barducci, A. Belyaev, M. Buchkremer, J. Marrouche, S. Moretti, L. Panizzi, Xqcat: extra quark combined analysis tool, *Comput. Phys. Commun.* 197 (2015) 263–275. [arXiv:1409.3116](https://arxiv.org/abs/1409.3116), [doi:10.1016/j.cpc.2015.08.003](https://doi.org/10.1016/j.cpc.2015.08.003).
- [26] E. Conte, B. Dumont, B. Fuks, C. Wymant, Designing and recasting lhc analyses with madanalysis 5, *Eur. Phys. J. C* 74 (2014) 3103. [arXiv:1405.3982](https://arxiv.org/abs/1405.3982), [doi:10.1140/epjc/s10052-014-3103-0](https://doi.org/10.1140/epjc/s10052-014-3103-0).
- [27] D. Dercks, N. Desai, J. S. Kim, K. Rolbiecki, J. Tattersall, T. Weber, Checkmate 2: From the model to the limit, *Comput. Phys. Commun.* 221 (2017) 383–418. [arXiv:1611.09856](https://arxiv.org/abs/1611.09856), [doi:10.1016/j.cpc.2017.08.021](https://doi.org/10.1016/j.cpc.2017.08.021).

- [28] F. Ambrogio, S. Kraml, S. Kulkarni, U. Laa, A. Lessa, V. Magerl, J. Sonnenveld, M. Traub, W. Waltenberger, Smodels v1.1 user manual: Improving simplified model constraints with efficiency maps, *Comput. Phys. Commun.* 227 (2018) 72–98. [arXiv:1701.06586](#), [doi:10.1016/j.cpc.2018.01.008](#).
- [29] M. Papucci, K. Sakurai, A. Weiler, L. Zeune, Fastlim: a fast lhc limit calculator, *Eur. Phys. J. C* 74 (2014) 3163. [arXiv:1402.0492](#), [doi:10.1140/epjc/s10052-014-3163-1](#).
- [30] A. Buckley, J. Butterworth, L. Corpe, D. Huang, P. Sun, New sensitivity of current lhc measurements to vector-like quarks, *SciPost Phys.* 9 (5) (2020) 069. [arXiv:2006.07172](#), [doi:10.21468/SciPostPhys.9.5.069](#).
- [31] F. del Aguila, M. Perez-Victoria, J. Santiago, Effective description of quark mixing, *Phys. Lett. B* 492 (2000) 98–106. [arXiv:hep-ph/0007160](#), [doi:10.1016/S0370-2693\(00\)01071-6](#).
- [32] M. Aaboud, et al., Search for pair production of vector-like top quarks in events with one lepton, jets, and missing transverse momentum in  $\sqrt{s} = 13$  TeV  $pp$  collisions with the ATLAS detector, *JHEP* 08 (2017) 052. [arXiv:1705.10751](#), [doi:10.1007/JHEP08\(2017\)052](#).
- [33] M. Aaboud, et al., Search for pair production of heavy vector-like quarks decaying to high- $p_T$  W bosons and b quarks in the lepton-plus-jets final state in  $pp$  collisions at  $\sqrt{s} = 13$  TeV with the ATLAS detector, *JHEP* 10 (2017) 141. [arXiv:1707.03347](#), [doi:10.1007/JHEP10\(2017\)141](#).
- [34] M. Aaboud, et al., Search for new phenomena in events with same-charge leptons and  $b$ -jets in  $pp$  collisions at  $\sqrt{s} = 13$  TeV with the ATLAS detector, *JHEP* 12 (2018) 039. [arXiv:1807.11883](#), [doi:10.1007/JHEP12\(2018\)039](#).
- [35] M. Aaboud, et al., Search for single production of vector-like quarks decaying into  $Wb$  in  $pp$  collisions at  $\sqrt{s} = 13$  TeV with the ATLAS detector, *JHEP* 05 (2019) 164. [arXiv:1812.07343](#), [doi:10.1007/JHEP05\(2019\)164](#).

- [36] G. Aad, et al., Search for single production of a vectorlike  $T$  quark decaying into a Higgs boson and top quark with fully hadronic final states using the ATLAS detector, Phys. Rev. D 105 (9) (2022) 092012. [arXiv:2201.07045](#), [doi:10.1103/PhysRevD.105.092012](#).
- [37] G. Aad, et al., Search for pair-produced vector-like top and bottom partners in events with large missing transverse momentum in pp collisions with the ATLAS detector, Eur. Phys. J. C 83 (8) (2023) 719. [arXiv:2212.05263](#), [doi:10.1140/epjc/s10052-023-11790-7](#).
- [38] M. Aaboud, et al., Search for pair production of up-type vector-like quarks and for four-top-quark events in final states with multiple  $b$ -jets with the ATLAS detector, JHEP 07 (2018) 089. [arXiv:1803.09678](#), [doi:10.1007/JHEP07\(2018\)089](#).
- [39] G. Aad, et al., Search for pair-production of vector-like quarks in pp collision events at  $\sqrt{s}=13$  TeV with at least one leptonically decaying  $Z$  boson and a third-generation quark with the ATLAS detector, Phys. Lett. B 843 (2023) 138019. [arXiv:2210.15413](#), [doi:10.1016/j.physletb.2023.138019](#).
- [40] G. Aad, et al., Search for single production of vector-like  $T$  quarks decaying into  $Ht$  or  $Zt$  in pp collisions at  $\sqrt{s} = 13$  TeV with the ATLAS detector, JHEP 08 (2023) 153. [arXiv:2305.03401](#), [doi:10.1007/JHEP08\(2023\)153](#).
- [41] G. Aad, et al., Search for singly produced vectorlike top partners in multilepton final states with 139 fb<sup>-1</sup> of pp collision data at  $\sqrt{s}=13$  TeV with the ATLAS detector, Phys. Rev. D 109 (11) (2024) 112012. [arXiv:2307.07584](#), [doi:10.1103/PhysRevD.109.112012](#).
- [42] G. Aad, et al., Search for new particles in final states with a boosted top quark and missing transverse momentum in proton-proton collisions at  $\sqrt{s} = 13$  TeV with the ATLAS detector, JHEP 05 (2024) 263. [arXiv:2402.16561](#), [doi:10.1007/JHEP05\(2024\)263](#).

- [43] G. Aad, et al., Search for pair-production of vector-like quarks in lepton+jets final states containing at least one b-tagged jet using the Run 2 data from the ATLAS experiment, Phys. Lett. B 854 (2024) 138743. [arXiv:2401.17165](#), [doi:10.1016/j.physletb.2024.138743](#).
- [44] M. Aaboud, et al., Search for large missing transverse momentum in association with one top-quark in proton-proton collisions at  $\sqrt{s} = 13$  TeV with the ATLAS detector, JHEP 05 (2019) 041. [arXiv:1812.09743](#), [doi:10.1007/JHEP05\(2019\)041](#).
- [45] Search for single production of vector-like quarks decaying into  $Wb$  in  $pp$  collisions at  $\sqrt{s} = 13$  TeV with the ATLAS detector (8 2016).
- [46] Search for new phenomena in  $t\bar{t}$  final states with additional heavy-flavour jets in  $pp$  collisions at  $\sqrt{s} = 13$  TeV with the ATLAS detector (9 2016).
- [47] Search for new physics using events with  $b$ -jets and a pair of same charge leptons in  $3.2 \text{ fb}^{-1}$  of  $pp$  collisions at  $\sqrt{s} = 13$  TeV with the ATLAS detector (6 2016).
- [48] G. Aad, et al., Search for single production of vector-like quarks decaying into  $Wb$  in  $pp$  collisions at  $\sqrt{s} = 8$  TeV with the ATLAS detector, Eur. Phys. J. C 76 (8) (2016) 442. [arXiv:1602.05606](#), [doi:10.1140/epjc/s10052-016-4281-8](#).
- [49] G. Aad, et al., Search for pair and single production of new heavy quarks that decay to a  $Z$  boson and a third-generation quark in  $pp$  collisions at  $\sqrt{s} = 8$  TeV with the ATLAS detector, JHEP 11 (2014) 104. [arXiv:1409.5500](#), [doi:10.1007/JHEP11\(2014\)104](#).
- [50] G. Aad, et al., Search for production of vector-like quark pairs and of four top quarks in the lepton-plus-jets final state in  $pp$  collisions at  $\sqrt{s} = 8$  TeV with the ATLAS detector, JHEP 08 (2015) 105. [arXiv:1505.04306](#), [doi:10.1007/JHEP08\(2015\)105](#).
- [51] G. Aad, et al., Analysis of events with  $b$ -jets and a pair of leptons of the same charge in  $pp$  collisions at  $\sqrt{s} = 8$  TeV with the ATLAS detector, JHEP 10 (2015) 150. [arXiv:1504.04605](#), [doi:10.1007/JHEP10\(2015\)150](#).

- [52] M. Aaboud, et al., Combination of the searches for pair-produced vector-like partners of the third-generation quarks at  $\sqrt{s} = 13$  TeV with the ATLAS detector, Phys. Rev. Lett. 121 (21) (2018) 211801. [arXiv:1808.02343](#), [doi:10.1103/PhysRevLett.121.211801](#).
- [53] G. Aad, et al., Search for vector-like  $B$  quarks in events with one isolated lepton, missing transverse momentum and jets at  $\sqrt{s} = 8$  TeV with the ATLAS detector, Phys. Rev. D 91 (11) (2015) 112011. [arXiv:1503.05425](#), [doi:10.1103/PhysRevD.91.112011](#).
- [54] G. Aad, et al., Combination of searches for singly produced vector-like top quarks in pp collisions at  $\sqrt{s} = 13$  TeV with the ATLAS detector (8 2024). [arXiv:2408.08789](#).
- [55] M. Aaboud, et al., Search for pair- and single-production of vector-like quarks in final states with at least one  $Z$  boson decaying into a pair of electrons or muons in  $pp$  collision data collected with the ATLAS detector at  $\sqrt{s} = 13$  TeV, Phys. Rev. D 98 (11) (2018) 112010. [arXiv:1806.10555](#), [doi:10.1103/PhysRevD.98.112010](#).
- [56] G. Aad, et al., Search for single-production of vector-like quarks decaying into  $Wb$  in the fully hadronic final state in  $pp$  collisions at  $\sqrt{s} = 13$  TeV with the ATLAS detector (9 2024). [arXiv:2409.20273](#).
- [57] G. Aad, et al., Search for single production of vector-like quarks decaying into  $W(\ell\nu)b$  in pp collisions at  $\sqrt{s} = 13$  TeV with the ATLAS detector, JHEP 12 (2025) 012. [arXiv:2506.15515](#), [doi:10.1007/JHEP12\(2025\)012](#).
- [58] Projected sensitivity for non-resonant production of vector leptoquarks and single production of vector-like  $T$  quarks in final states with b-jets with the ATLAS experiment at the HL-LHC (10 2025).
- [59] M. Aaboud, et al., Search for pair production of heavy vector-like quarks decaying into hadronic final states in  $pp$  collisions at  $\sqrt{s} = 13$  TeV with the ATLAS detector, Phys. Rev. D 98 (9) (2018) 092005. [arXiv:1808.01771](#), [doi:10.1103/PhysRevD.98.092005](#).

- [60] M. Aaboud, et al., Search for top squarks in final states with one isolated lepton, jets, and missing transverse momentum in  $\sqrt{s} = 13$  TeV  $pp$  collisions with the ATLAS detector, Phys. Rev. D 94 (5) (2016) 052009. [arXiv:1606.03903](#), [doi:10.1103/PhysRevD.94.052009](#).
- [61] G. Aad, et al., Search for pair production of heavy top-like quarks decaying to a high- $p_T$   $W$  boson and a  $b$  quark in the lepton plus jets final state at  $\sqrt{s}=7$  TeV with the ATLAS detector, Phys. Lett. B 718 (2013) 1284–1302. [arXiv:1210.5468](#), [doi:10.1016/j.physletb.2012.11.071](#).
- [62] G. Aad, et al., Search for pair production of a heavy up-type quark decaying to a  $W$  boson and a  $b$  quark in the lepton+jets channel with the ATLAS detector, Phys. Rev. Lett. 108 (2012) 261802. [arXiv:1202.3076](#), [doi:10.1103/PhysRevLett.108.261802](#).
- [63] G. Aad, et al., Search for single vector-like  $B$  quark production and decay via  $B \rightarrow bH(b\bar{b})$  in  $pp$  collisions at  $\sqrt{s} = 13$  TeV with the ATLAS detector, JHEP 11 (2023) 168. [arXiv:2308.02595](#), [doi:10.1007/JHEP11\(2023\)168](#).
- [64] M. Aaboud, et al., Search for pair production of heavy vector-like quarks decaying into high- $p_T$   $W$  bosons and top quarks in the lepton-plus-jets final state in  $pp$  collisions at  $\sqrt{s} = 13$  TeV with the ATLAS detector, JHEP 08 (2018) 048. [arXiv:1806.01762](#), [doi:10.1007/JHEP08\(2018\)048](#).
- [65] G. Aad, et al., Search for the production of single vector-like and excited quarks in the  $Wt$  final state in  $pp$  collisions at  $\sqrt{s} = 8$  TeV with the ATLAS detector, JHEP 02 (2016) 110. [arXiv:1510.02664](#), [doi:10.1007/JHEP02\(2016\)110](#).
- [66] A. Tumasyan, et al., Search for single production of a vector-like  $T$  quark decaying to a top quark and a  $Z$  boson in the final state with jets and missing transverse momentum at  $\sqrt{s} = 13$  TeV, JHEP 05 (2022) 093. [arXiv:2201.02227](#), [doi:10.1007/JHEP05\(2022\)093](#).
- [67] A. M. Sirunyan, et al., Search for electroweak production of a vector-like quark decaying to a top quark and a Higgs boson using boosted

- topologies in fully hadronic final states, JHEP 04 (2017) 136. [arXiv:1612.05336](#), [doi:10.1007/JHEP04\(2017\)136](#).
- [68] V. Khachatryan, et al., Search for single production of a heavy vector-like T quark decaying to a Higgs boson and a top quark with a lepton and jets in the final state, Phys. Lett. B 771 (2017) 80–105. [arXiv:1612.00999](#), [doi:10.1016/j.physletb.2017.05.019](#).
- [69] A. M. Sirunyan, et al., Search for pair production of vector-like T and B quarks in single-lepton final states using boosted jet substructure in proton-proton collisions at  $\sqrt{s} = 13$  TeV, JHEP 11 (2017) 085. [arXiv:1706.03408](#), [doi:10.1007/JHEP11\(2017\)085](#).
- [70] A. Tumasyan, et al., Search for a vector-like quark  $T' \rightarrow tH$  via the diphoton decay mode of the Higgs boson in proton-proton collisions at  $\sqrt{s} = 13$  TeV, JHEP 09 (2023) 057. [arXiv:2302.12802](#), [doi:10.1007/JHEP09\(2023\)057](#).
- [71] A. Hayrapetyan, et al., Search for production of a single vector-like quark decaying to  $tH$  or  $tZ$  in the all-hadronic final state in pp collisions at  $\sqrt{s} = 13$  TeV (5 2024). [arXiv:2405.05071](#).
- [72] A. M. Sirunyan, et al., Search for electroweak production of a vector-like T quark using fully hadronic final states, JHEP 01 (2020) 036. [arXiv:1909.04721](#), [doi:10.1007/JHEP01\(2020\)036](#).
- [73] A. M. Sirunyan, et al., Search for single production of a vector-like T quark decaying to a Z boson and a top quark in proton-proton collisions at  $\sqrt{s} = 13$  TeV, Phys. Lett. B 781 (2018) 574–600. [arXiv:1708.01062](#), [doi:10.1016/j.physletb.2018.04.036](#).
- [74] Search for pair production of vector-like T quarks in the lepton plus jets final state (2016).
- [75] S. Chatrchyan, et al., Inclusive Search for a Vector-Like T Quark with Charge  $\frac{2}{3}$  in pp Collisions at  $\sqrt{s} = 8$  TeV, Phys. Lett. B 729 (2014) 149–171. [arXiv:1311.7667](#), [doi:10.1016/j.physletb.2014.01.006](#).

- [76] S. Chatrchyan, et al., Search for Pair Produced Fourth-Generation Up-Type Quarks in  $pp$  Collisions at  $\sqrt{s} = 7$  TeV with a Lepton in the Final State, *Phys. Lett. B* 718 (2012) 307–328. [arXiv:1209.0471](#), [doi:10.1016/j.physletb.2012.10.038](#).
- [77] A. M. Sirunyan, et al., Search for vector-like T and B quark pairs in final states with leptons at  $\sqrt{s} = 13$  TeV, *JHEP* 08 (2018) 177. [arXiv:1805.04758](#), [doi:10.1007/JHEP08\(2018\)177](#).
- [78] A. Tumasyan, et al., Search for pair production of vector-like quarks in leptonic final states in proton-proton collisions at  $\sqrt{s} = 13$  TeV, *JHEP* 07 (2023) 020. [arXiv:2209.07327](#), [doi:10.1007/JHEP07\(2023\)020](#).
- [79] A. M. Sirunyan, et al., Search for single production of vector-like quarks decaying to a Z boson and a top or a bottom quark in proton-proton collisions at  $\sqrt{s} = 13$  TeV, *JHEP* 05 (2017) 029. [arXiv:1701.07409](#), [doi:10.1007/JHEP05\(2017\)029](#).
- [80] A. Hayrapetyan, et al., Search for single production of a vector-like T quark decaying to a top quark and a neutral scalar boson in the lepton+jets final state in proton-proton collisions at  $\sqrt{s} = 13$  TeV (10 2025). [arXiv:2510.25874](#).
- [81] A. Hayrapetyan, et al., Review of searches for vector-like quarks, vector-like leptons, and heavy neutral leptons in proton–proton collisions at  $\sqrt{s}=13$  TeV at the CMS experiment, *Phys. Rept.* 1115 (2025) 570–677. [arXiv:2405.17605](#), [doi:10.1016/j.physrep.2024.09.012](#).
- [82] A. M. Sirunyan, et al., Search for vector-like quarks in events with two oppositely charged leptons and jets in proton-proton collisions at  $\sqrt{s} = 13$  TeV, *Eur. Phys. J. C* 79 (4) (2019) 364. [arXiv:1812.09768](#), [doi:10.1140/epjc/s10052-019-6855-8](#).
- [83] A. M. Sirunyan, et al., Search for single production of vector-like quarks decaying into a b quark and a W boson in proton-proton collisions at  $\sqrt{s} = 13$  TeV, *Phys. Lett. B* 772 (2017) 634–656. [arXiv:1701.08328](#), [doi:10.1016/j.physletb.2017.07.022](#).

- [84] A. M. Sirunyan, et al., Search for pair production of vector-like quarks in the  $bW\bar{b}W$  channel from proton-proton collisions at  $\sqrt{s} = 13$  TeV, Phys. Lett. B 779 (2018) 82–106. [arXiv:1710.01539](#), [doi:10.1016/j.physletb.2018.01.077](#).
- [85] A. M. Sirunyan, et al., Search for pair production of vectorlike quarks in the fully hadronic final state, Phys. Rev. D 100 (7) (2019) 072001. [arXiv:1906.11903](#), [doi:10.1103/PhysRevD.100.072001](#).
- [86] V. Khachatryan, et al., Search for vector-like charge 2/3 T quarks in proton-proton collisions at  $\sqrt{s} = 8$  TeV, Phys. Rev. D 93 (1) (2016) 012003. [arXiv:1509.04177](#), [doi:10.1103/PhysRevD.93.012003](#).
- [87] S. Chatrchyan, et al., Search for Heavy, Top-Like Quark Pair Production in the Dilepton Final State in  $pp$  Collisions at  $\sqrt{s} = 7$  TeV, Phys. Lett. B 716 (2012) 103–121. [arXiv:1203.5410](#), [doi:10.1016/j.physletb.2012.07.059](#).
- [88] V. Khachatryan, et al., Search for vector-like T quarks decaying to top quarks and Higgs bosons in the all-hadronic channel using jet substructure, JHEP 06 (2015) 080. [arXiv:1503.01952](#), [doi:10.1007/JHEP06\(2015\)080](#).
- [89] A. M. Sirunyan, et al., Search for single production of vector-like quarks decaying to a b quark and a Higgs boson, JHEP 06 (2018) 031. [arXiv:1802.01486](#), [doi:10.1007/JHEP06\(2018\)031](#).
- [90] A. Tumasyan, et al., Search for a heavy resonance decaying into a top quark and a W boson in the lepton+jets final state at  $\sqrt{s} = 13$  TeV, JHEP 04 (2022) 048. [arXiv:2111.10216](#), [doi:10.1007/JHEP04\(2022\)048](#).
- [91] A. Hayrapetyan, et al., A search for bottom-type vector-like quark pair production in dileptonic and fully hadronic final states in proton-proton collisions at  $\sqrt{s} = 13$  TeV (2 2024). [arXiv:2402.13808](#).
- [92] A. M. Sirunyan, et al., A search for bottom-type, vector-like quark pair production in a fully hadronic final state in proton-proton collisions

- at  $\sqrt{s} = 13$  TeV, Phys. Rev. D 102 (2020) 112004. [arXiv:2008.09835](#), [doi:10.1103/PhysRevD.102.112004](#).
- [93] V. Khachatryan, et al., Search for pair-produced vectorlike B quarks in proton-proton collisions at  $\sqrt{s}=8$  TeV, Phys. Rev. D 93 (11) (2016) 112009. [arXiv:1507.07129](#), [doi:10.1103/PhysRevD.93.112009](#).
- [94] A. M. Sirunyan, et al., Search for single production of vector-like quarks decaying to a top quark and a W boson in proton-proton collisions at  $\sqrt{s} = 13$  TeV, Eur. Phys. J. C 79 (2019) 90. [arXiv:1809.08597](#), [doi:10.1140/epjc/s10052-019-6556-3](#).
- [95] A. M. Sirunyan, et al., Search for top quark partners with charge 5/3 in the same-sign dilepton and single-lepton final states in proton-proton collisions at  $\sqrt{s} = 13$  TeV, JHEP 03 (2019) 082. [arXiv:1810.03188](#), [doi:10.1007/JHEP03\(2019\)082](#).